MNRAS **000**, 1–17 (2011) Preprint 21 May 2019 Compiled using MNRAS LATEX style file v3.0

High-frequencies in *TESS* A–F main sequence stars

L. A. Balona[1], D. L. Holdsworth[2], M. S. Cunha[3]
[1] *South African Astronomical Observatory, P.O. Box 9, Observatory, Cape Town, South Africa*
[2] *Jeremiah Horrocks Institute, University of Central Lancashire, Preston PR1 2HE, UK*
[3] *Instituto de Astrofísica e Ciências do Espaço, Universidade do Porto, CAUP, Rua das Estrelas, PT4150-762 Porto, Portugal*

Accepted .... Received ...

ABSTRACT
The driving mechanism for high-frequency oscillations in some chemically peculiar Ap stars, the roAp stars, is not understood. The *TESS* data provide an ideal opportunity to extend the number of roAp stars which might provide further clues to address this problem. From an examination of over 18000 stars in *TESS* sectors 1–7, we have discovered high-frequency pulsations in 14 A–F stars, of which only 3 are classified as Ap stars. In addition to these new discoveries, we discuss the frequencies in 9 previously known roAp stars. In one of these stars, HD 60435, we confirm a previous finding that the pulsations have lifetimes of only a few days. In another known roAp star, HD 6532, the relative amplitudes of the rotationally-modulated sidelobes, which are generally used to estimate the inclination of the magnetic axis relative to the rotational axis, are significantly different from those found in ground-based B-band photometric observations. We also discuss 4 δ Scuti stars which appear to have independent frequencies similar to those of roAp stars.

Key words: stars:oscillations; stars: chemically peculiar

1 INTRODUCTION

The Ap stars have non-uniform distributions of chemical abundances on their surfaces and strong, predominantly dipolar, magnetic fields. The magnetic poles do not generally coincide with the axis of rotation, resulting in a variation of the observed mean magnetic field strength, as well as light and spectral line profiles variations, with the period of rotation. Kurtz (1978, 1982) discovered that while most of the Ap stars do not show any oscillations, some cool Ap stars exhibit remarkable single or multiperiodic pulsations with periods in the range 4–24 min. These are the rapidly oscillating Ap stars (roAp stars).

The high-frequency pulsation modes in roAp stars are not predicted to be excited in standard models, but driving by the κ mechanism in the H/HeI partial ionization zone is almost enough to overcome damping in the rest of the star. Driving of high-frequency oscillations similar to those observed in roAp stars is possible if a temperature inversion is present in the lower atmosphere (Gautschy et al. 1998). The temperature inversion, which need only be 1000–3000 K, raises the superficial critical frequency sufficiently to reflect the high-frequency modes. A temperature inversion of about 500-1000 K may also explain the abnormal profiles of the hydrogen Balmer lines (the core-wing anomaly) in some cool Ap stars (Kochukhov et al. 2002).

In another approach to the problem, Balmforth et al. (2001) noted that the vertical magnetic field at the poles has the effect of suppressing convection. With convection suppressed, pulsational driving in the magnetic polar regions by the κ mechanism is sufficiently strong to overcome damping in other parts of the star. This model explains, in a natural way, why the oscillations have a preferred spherical harmonic axis closely aligned with the magnetic axis and not the rotational axis. It is presumed that non-axisymmetric modes are damped. The result is a modulation in the amplitude of the axisymmetric modes with the period of rotation, as observed in many roAp stars.

A fundamental problem in understanding the roAp stars is their location in the H-R diagram. Cunha (2002) used models similar to those of Balmforth et al. (2001) to determine the red and blue edges of the theoretical instability strip. However, a significant fraction of roAp stars are cooler than the predicted red edge.

The strong magnetic field in a roAp star leads to pulsation frequencies which are shifted with respect to those in a non-magnetic star (Dziembowski & Goode 1996; Bigot & Dziembowski 2002; Cunha & Gough 2000; Saio & Gautschy 2004; Cunha 2006). The oscillations are damped by the leakage of pulsation energy due to magnetic slow waves. Slow-wave damping is enough to stabilize low-order (δ Scuti type) pulsations (Saio 2005). However, helium depletion by diffusion might also play an important role in the stability of low-order modes in roAp stars (Cunha et al. 2004). The strong magnetic field also leads to the presence of compressible Alfvén waves in the atmosphere and forces

the acoustic waves to move along the magnetic field lines. As a result, the acoustic critical frequency decreases as the field lines become inclined and energy is lost through running waves. On the other hand, the magnetic waves are refracted, ensuring that part of the wave energy is kept inside the star, potentially allowing for the existence of oscillations of arbitrarily high frequency (Sousa & Cunha 2008). Indeed, for many roAp stars the observed frequencies are higher than the calculated cut-off frequency (Saio et al. 2010; Saio 2014; Holdsworth et al. 2018).

The roAp stars need to be investigated in the context of other pulsating stars within the same instability region in the H-R diagram, i.e. the δ Sct and γ Dor stars. Space observations have shown that current models of these stars, which are certainly simpler to understand than the roAp stars, are inadequate. The greatest discrepancy is that the models are unable to account for the low frequencies which are characteristic of at least 98 percent of δ Sct stars (Balona 2018a,b, but see Bowman 2017; Bowman & Kurtz 2018). It seems that the effect of convection is important even for the hottest stars, though models which include convection are still unable to match the observations (Antoci et al. 2014; Xiong et al. 2016; Balona 2018a,b). The δ Sct and γ Dor stars co-exist in the same region of the H-R diagram along with non-pulsating stars (Balona 2018a). The difference in frequency spectra appears to be due to different mode selection from star to star. It seems that mode selection differs widely, even for stars with the same effective temperature and luminosity. Another unforeseen problem is that a large fraction of the A stars seem to have spots (Balona 2013, 2017). About 15 percent of the A stars have an additional broad feature in the periodogram at a frequency slightly lower than the rotational frequency which can be possibly understood as due to Rossby waves (Saio et al. 2018). Our current understanding of the outer layers of stars with radiative atmospheres may therefore need revision. This clearly impacts on the roAp stars.

The Transiting Exoplanet Survey Satellite mission (*TESS*; Ricker et al. 2015) is designed to search for exoplanets. It is also an excellent tool to search for roAp stars among a very large population of normal and peculiar A–F stars. The aim of this paper is to present some newly-discovered roAp and roAp-like stars. A report on the first discoveries of roAp stars by *TESS* has been presented by Cunha et al. (2019). By extending the number of roAp stars, the instability region becomes better defined and will provide an important constraint on the models. Furthermore, the different pulsational properties will hopefully provide insights into the driving mechanism. While the majority of stars with high frequencies discovered by *TESS* are not known to be Ap stars, it is expected that spectroscopic observations will confirm that chemical peculiarities are present.

2 WHAT IS A ROAP STAR?

In the past there has never been any problem in classifying a star as roAp. As its name implies, it is simply an Ap star in which high radial order oscillations, i.e. higher radial order than that expected from δ Sct stars, are observed. The advent of space photometry is slowly revealing stars which seem to have pulsations in the roAp frequency range, but which are not known Ap stars (e.g. Balona et al. 2012; Cunha et al. 2019). It is possible that the stars may have simply been mis-classified and that they are, indeed, magnetic and chemically peculiar. They might also be composite systems in which the high frequencies originate in another star. Nevertheless, until these points have been clarified, it cannot be stated with certainty that roAp-like pulsations are restricted to chemically peculiar stars. It is thus important to continue to look for high frequencies in apparently normal stars as well as known Ap stars.

Another problem concerns the detection of frequencies in the roAp range in δ Sct stars. In the case of the known roAp star HD 218994, for example, it is assumed that the δ Sct pulsations occur in one star while the other star in this close double is the Ap star responsible for the high-frequencies (Kurtz et al. 2008). This explanation is possible, of course, but it may be incorrect. For example, Holdsworth et al. (2014) found 13 δ Sct stars with pulsations extending to above 65 d^{-1}, all being classified as metallic-lined (Am) stars rather than Ap stars. However, they caution that at low spectral resolutions it is difficult to discriminate between Am and Ap stars. KIC 4840675, a δ Sct star with independent frequencies in the range 118–129 d^{-1} (Balona et al. 2012), is another example of an apparently non-peculiar star exhibiting high-frequency pulsations.

In this context it is important to keep in mind that the δ Sct and roAp phenomena cover a wide range of effective temperatures and luminosities in the H-R diagram. Consequently, similar oscillation frequencies may correspond to rather different radial orders, n, in two different stars and hence to perturbations that are significantly different.

The radial order of a pulsation can be estimated from the pulsation frequencies and the global stellar parameters. We have carried out this exercise for all roAp stars known prior to the *TESS* launch. Masses were estimated from the scaling proposed by Eker et al. (2015) and radii derived from the effective temperatures and luminosities. The mean density was then used to estimate the large frequency separation, scaling from the solar value. Finally, the radial order, n, was estimated by dividing the frequency of the mode with highest amplitude by the large frequency separation. For the known roAp stars, the radial order is typically in the range $20 \leq n \leq 40$, with some stars having modes with radial order as low as $n \approx 15$ and others as high as high as $n \approx 70$. These radial orders are different from those expected in typical δ Sct stars. However, pulsations higher than radial order $n = 15$ have been found in some δ Sct stars and their excitation explained by a turbulent pressure driving mechanism (Antoci et al. 2014). Since the radial order numbers provide a scaled version of the observed frequencies, they may prove more useful when comparing acoustic pulsations in stars across the instability strip.

We have examined all 211 known SrEuCr and Si Ap/Bp stars in *TESS* sectors 1–7 that are listed in the catalogue of chemically peculiar stars by Ghazaryan et al. (2018). Whereas 42 stars show no significant variability, 60 are δ Sct stars, 10 are γ Dor and 9 are eclipsing variables. The majority, 88, are rotational variables. Among these chemically peculiar stars there are 11 known roAp stars, i.e. members of the 61 stars listed by Smalley et al. (2015). Two of the five high-frequency pulsators discovered by Cunha et al. (2019) are known Ap stars. A further three Ap stars are discovered

Table 1. Stars exhibiting high frequencies in *TESS* sectors 1–7. The TIC number, name, sector and rotational frequency is listed in the first four columns. The V magnitude, adopted effective temperature, $T_{\rm eff}$, and source reference for $T_{\rm eff}$ follows. Finally, the luminosity from the *GAIA* DR2 parallax and spectral type is listed. For TIC 100775380 the *Hipparcos* parallax has been used.

TIC	Name	Sectors	$\nu_{\rm rot}$ $\rm d^{-1}$	V mag	$T_{\rm eff}$ K	Ref	$\log \frac{L}{L_\odot}$	Spectral Type
Known roAp stars:								
33601621	HD 42659	6	0.3758	6.75	7449	7	1.55	A3SrCrEu
41259805	HD 43226	1–7	0.5833	8.94	8293	11	1.25	A0SrEu
136842396	HD 9289	3	0.1169	9.38	7840	3	0.87	A3SrEuCr
167695608	TYC 8912-1407-1	1–4,6,7		11.51	7460	11	1.29	ApSrEu(Cr)
268751602	HD 12932	3		10.17	7542	1		ApSrEuCr
279485093	HD 24712	5	0.0803	6.00	7235	8	0.92	kA5mF0V?Sr
326185137	HD 6532	3	0.5137	8.40	7900	2	1.21	ApSrCrEu
340006157	HD 60435	3,6,7	0.1302	8.89	7800	2	1.28	A3SrEu
350146296	HD 63087	1–7	0.3754	9.41	7450	11	0.97	A7IV
New roAp stars:								
17676722	HD 63773	7	0.6254	8.70	8549	12	1.25	A2
156886111	HD 47284	6,7	0.1459	9.29	7417	6	1.36	A5SiEuCr
259587315	HD 30849	4,5	0.0632	8.85	7653	4	1.53	ApSrCrEu
349945078	HD 57040	6,7	0.0371	9.24	7516	6	1.13	A2EuSr?
Candidate roAp stars:								
3814749	HD 3748	3	0.5920	9.20	7750	4	1.12	A0/1IV/V + A9/F0
49818005	HD 19687	4		9.70	6829	1	0.89	A3
92350273	CD-33 15279	1		9.96	7235	1	1.58	F5
220073982	HD 288081	6	3.2600	10.09	8064	10	1.45	A2
300908057	HD 203997	1		9.21	6992	1	0.31	G1V
391892593	HD 63037	1–7		9.67	6873	1	1.04	A3mA8-F0, A3:+F0:
Additional high-frequency pulsators:								
100775380	HD 39763	5,6		7.75	8420	9	1.49	A1V
308307808	CD-60 2021	4,7		10.40	7735	6	1.20	A3:, A5
399665133	BD+06 763	5	2.2370	9.25	7915	6	1.28	A2
407661867	HD 37584	1–7	1.7770	8.33	8750	11	1.22	A3V
High frequencies in δ Scuti stars:								
98728812	HD 18407	4		8.92	8483	6	1.31	A0V
302296720	HD 203144	1		8.65	6968	1	0.85	A5/7V
317719322	HD 40098	6		8.53	8366	6	1.21	A2/3V
439399707	HD 225186	2	0.6016	9.01	8000	1	1.06	A3V

References:
1 - Stevens et al. (2017); 2 - Elkin et al. (2008); 3 - Ryabchikova et al. (2007); 4 - Kunder et al. (2017);
5 - Netopil et al. (2017); 6 -McDonald et al. (2017); 7 - Muñoz Bermejo et al. (2013); 8 - Perraut et al. (2016);
9 -Chandler et al. (2016); 10 - Kounkel et al. (2018); 11 - Cunha et al. (2019); 12 - Stassun et al. (2018).

as roAp in this work. Thus 16 of the 211 chemically peculiar stars in *TESS* sectors 1–7 are confirmed roAp stars.

Because of the unexpected detection of roAp-like oscillations in stars classified as non-peculiar (but likely misclassified) stars, we define a potential roAp star as any A or F star with independent frequencies exceeding $60\,\rm d^{-1}$. These are frequencies which are not a result of non-linear combinations of lower-frequency parent modes. Note that pulsating subdwarfs have frequencies in the roAp range and some of these were encountered during the course of inspection of *TESS* data. A literature search is usually sufficient to identify subdwarfs. The stars described here are not known subdwarfs, as can be inferred from their luminosities.

3 DATA AND ANALYSIS

TESS observes 26 partially overlapping sectors of the sky, each for approximately one month. Light curves are generated with two-minute cadence using simple aperture photometry (SAP) and pre-search data conditioning (PDC). The PDC pipeline module uses singular value decomposition to identify and correct for time-correlated instrumental signatures in the light curves. In addition, PDC corrects the flux for each target to account for the effects of crowding from other stars. Only PDC light curves are used in this paper. A description of how these data products were generated is provided by Jenkins et al. (2016). It should be noted that long-term variations are difficult to correct and although PDC light curves provide the best estimate of the true light curve, unexpected deviations may occur. This will not affect

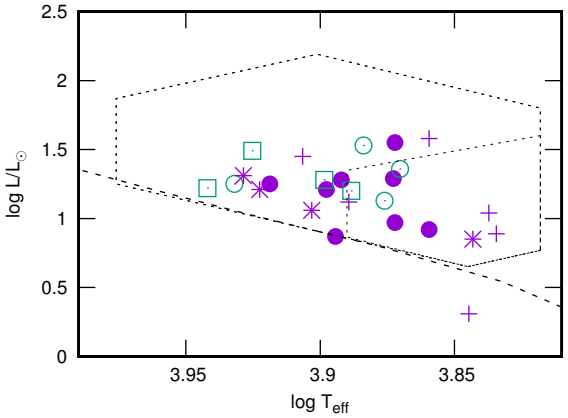

Figure 1. Location of the stars in Table 1 in the theoretical H–R diagram. Filled circles: known roAp stars; open circles: new roAp stars; crosses: candidate roAp stars; squares: additional high-frequency pulsators; asterisks: high frequencies in δ Sct stars. The large polygon is the observed instability region for δ Sct stars while the smaller polygon shows where both δ Sct and γ Dor stars are located (Balona 2018a). The dashed line is the zero-age main sequence from solar abundance models by Bertelli et al. (2008).

the high frequencies, but distortions in the rotational light curve can be expected, especially for long periods.

The *TESS* input catalogue (Stassun et al. 2018) lists stellar parameters for stars observed by *TESS*. These were obtained from multicolour photometry or, if available, spectroscopic estimates from the literature. The effective temperatures, $T_{\rm eff}$, of Ap stars are, in general, poorly known because the line blanketing caused by the chemical peculiarities leads to unreliable estimates of $T_{\rm eff}$ from multicolour photometry.

The stars selected for analysis were observed in sectors 1–7. All stars with effective temperatures $T_{\rm eff} \geq 6000$ K were chosen. Lomb-Scargle periodograms up to the Nyquist limit of about 360 $\rm d^{-1}$ were calculated. From visual examination of the light curves and periodograms, each star was assigned a variability type, if appropriate, using the definitions in the *General Catalogue of Variable Stars* (Samus et al. 2009) as a guide. In this way, stars with strange frequency distributions or high frequencies could be noted for further examination. This list included not only Ap stars, but apparently chemically normal stars and some δ Scuti stars with frequencies within the roAp range. Over 18000 stars were examined in this way.

Note that the photometric aperture in *TESS* is large (but similar to the aperture size used in ground-based photoelectric photometry). The chance of contamination by a star of similar brightness is therefore not negligible. For this reason, the field of each star was inspected using the images provided in the SIMBAD database. When contamination is a possibility it is noted in the text.

In some candidate stars, a mean-light variation associated with rotation was present. The rotational frequency was found by fitting a truncated Fourier series plus a polynomial to the data and selecting the frequency which gives the best fit. In order to study the high frequencies, the fitted rotational light curve was subtracted from the data before calculating the periodogram. The false alarm probability criterion (Scargle 1982) was used to assess the significance of a frequency peak.

The list of candidates is shown in Table 1. The stars from sectors 1 and 2 that are discussed by Cunha et al. (2019) are not included here except for a few where additional data is available from the other sectors. In this table the stellar luminosities were derived from *GAIA* DR2 parallaxes (Gaia Collaboration et al. 2016, 2018). The bolometric correction was obtained from $T_{\rm eff}$ using the calibration of Pecaut & Mamajek (2013). The reddening correction was derived from a three-dimensional reddening map by Gontcharov (2017). The theoretical H–R diagram is shown in Fig. 1.

4 KNOWN ROAP STARS IN SECTORS 3–7

In this section we discuss stars which are known to be roAp and observed by *TESS*. This includes 3 stars in *TESS* sectors 1 and 2 previously discussed by Cunha et al. (2019), but with additional data from later sectors. Note that frequency units of cycles per day ($\rm d^{-1}$) and relative brightness of parts per thousand (ppt) are used throughout this paper.

4.1 TIC 33601621 (HD 42659)

The very low amplitude roAp pulsations in this star were announced by Martinez et al. (1993). The pulsations seem to vary in amplitude and were not visible at times. Martinez & Kurtz (1994a) estimated the frequency to be around 150.0 $\rm d^{-1}$. Hartmann & Hatzes (2015) found the star to be a spectroscopic binary with an orbital period of 93.2 d.

The star was observed for 22.7 d in sector 6. The periodogram in Fig. 2 shows three peaks: $\nu_1 = 150.99 \pm 0.03$, $A_1 = 0.038 \pm 0.009$, $\nu_2 = 150.61 \pm 0.03$, $A_2 = 0.034 \pm 0.009$ and $\nu_3 = 151.36 \pm 0.04\,\rm d^{-1}$, $A_3 = 0.027 \pm 0.009$ ppt. The mean light rotational curve has a frequency of $\nu_{\rm rot} = 0.3758 \pm 0.0003\,\rm d^{-1}$ (Fig. 2). The triplet in the frequency spectrum is not due to three independent frequencies, but a result of rotational amplitude modulation of the only real frequency, ν_1.

4.2 TIC 41259805 (HD 43226)

This known Ap star was discovered to be a rapid oscillator by Cunha et al. (2019) from sector 1 and 2 observations. Here we analyze the data for sectors 1–7. The star has only a single frequency at $\nu_1 = 199.673 \pm 0.003\,\rm d^{-1}$, amplitude $A_1 = 0.040 \pm 0.006$ ppt (Fig. 3). Cunha et al. (2019) find an additional peak at $\nu_1 - \nu_{\rm rot} = 199.087\,\rm d^{-1}$ with S/N = 4.7, but this is not visible with the additional data now available. The rotational light curve frequency is refined to $\nu_{\rm rot} = 0.58326 \pm 0.00001\,\rm d^{-1}$.

4.3 TIC 136842396 (HD 9289)

Kurtz et al. (1994) discovered that HD 9289 pulsates with three frequencies in the range 134–139 $\rm d^{-1}$. Observations from the *MOST* satellite were analysed by Gruberbauer et al. (2011) who found frequencies of 136.938, 136.704, 137.175, 135.931, 135.814 and 136.281 $\rm d^{-1}$, which

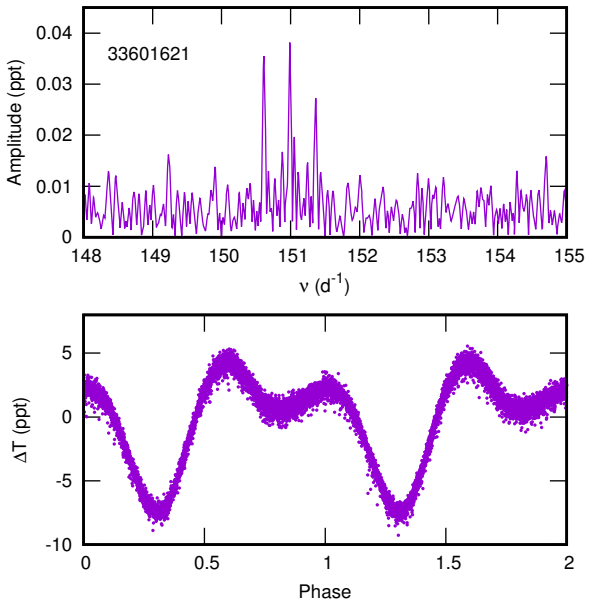

Figure 2. Periodogram of TIC 33601621 and the light curve phased with $\nu_{\rm rot} = 0.3758\,{\rm d}^{-1}$. ΔT is the relative *TESS* intensity in parts per thousand.

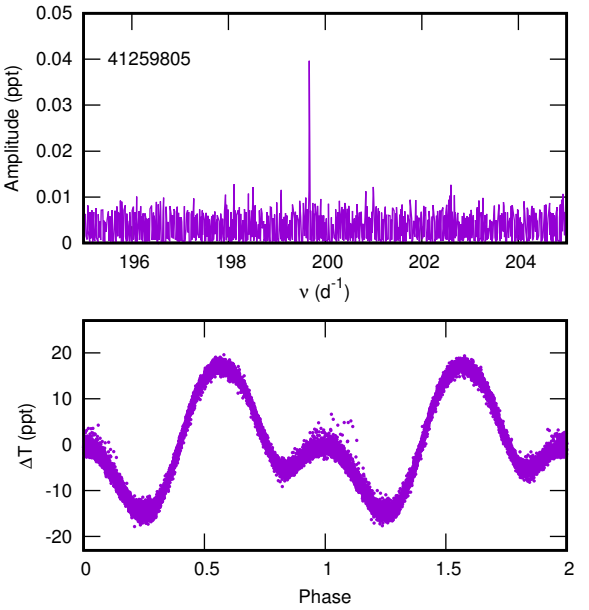

Figure 3. Periodogram of TIC 41259805 and the light curve phased with $\nu_{\rm rot} = 0.58326\,{\rm d}^{-1}$.

do not quite match those found by Kurtz et al. (1994). Aliasing was considered as a possible solution, but the different results might just as well stem from an intrinsic change in the pulsation behaviour of the star.

Gruberbauer et al. (2011) obtained a rotational frequency of $0.1166\,{\rm d}^{-1}$ from the mean light curve, or $0.1176\,{\rm d}^{-1}$ from the pulsational sidelobes. The *TESS* data span 20.3 d which covers only two cycles. Moreover, the PDC long-term correction algorithm has clearly introduced a distortion. For this reason the raw data were used to

Table 2. Extracted frequencies (ν in ${\rm d}^{-1}$) and amplitudes (A in ppt) for TIC 136842396.

ID	ν	A
ν_1	134.126 ± 0.023	0.05 ± 0.02
ν_2	135.815 ± 0.026	0.04 ± 0.02
$\nu_2 + \nu_{\rm rot}$	135.928 ± 0.019	0.06 ± 0.02
$\nu_3 - 2\nu_{\rm rot}$	136.710 ± 0.014	0.08 ± 0.02
ν_3	136.941 ± 0.005	0.24 ± 0.02
$\nu_3 + 2\nu_{\rm rot}$	137.176 ± 0.020	0.05 ± 0.02
ν_4	139.458 ± 0.012	0.09 ± 0.02
$\nu_4 + 2\nu_{\rm rot}$	139.695 ± 0.014	0.08 ± 0.02

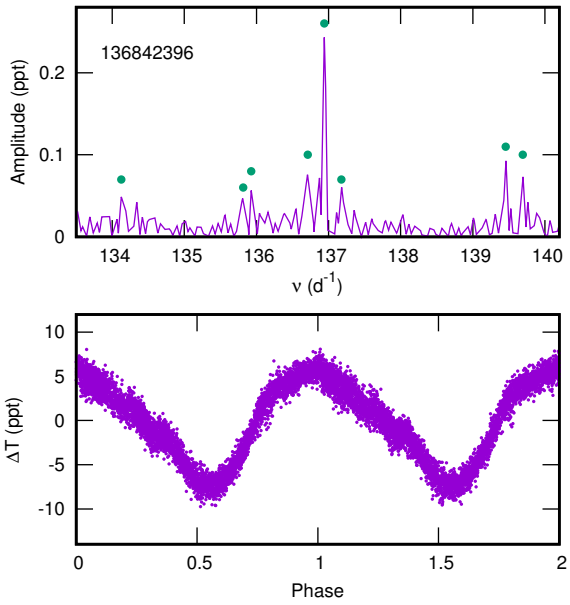

Figure 4. Periodogram of TIC 136842396 and the light curve phased with $\nu_{\rm rot} = 0.1169\,{\rm d}^{-1}$. The dots in the periodogram indicate the extracted frequencies.

examine the rotation curve. From the raw data we find $\nu_{\rm rot} = 0.1169 \pm 0.0003\,{\rm d}^{-1}$.

Frequencies extracted from the *TESS* data are listed in Table 2. Both the frequencies and the relative amplitudes are in good agreement with those reported in Gruberbauer et al. (2011). Three new peaks are visible in the *TESS* data at 134.126, 139.458 and $139.695\,{\rm d}^{-1}$. On the other hand, the peak at $136.281\,{\rm d}^{-1}$ cited by Gruberbauer et al. (2011) is not visible.

It is possible to identify some rotational multiplets as shown in Table 2, which means that there are only four physical modes, ν_1, ν_2, ν_3 and ν_4. A peak at $134.344\,{\rm d}^{-1}$, although not formally significant, could possibly be identified as an additional multiplet $\nu_1 + 2\nu_{\rm rot}$. Fig. 4 shows the periodogram and rotational light curve.

4.4 TIC 167695608 (TYC 8912-1407-1)

This star is J0651 in the work of Holdsworth et al. (2014), who found a pulsation frequency of $132.38\,{\rm d}^{-1}$ with no clear indications of rotational modulation in the light curve. Sec-

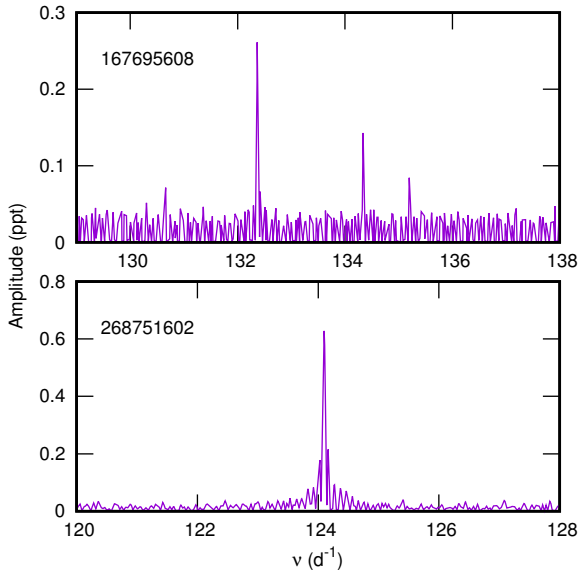

Figure 5. Periodograms for TIC 167695608 and TIC 268751602.

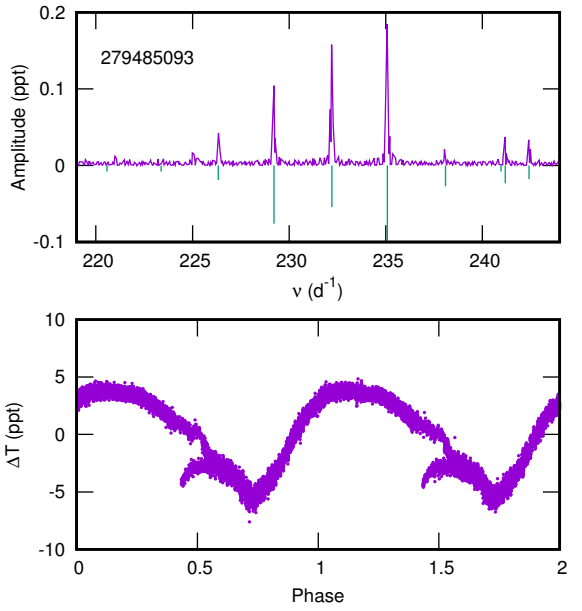

Figure 6. Periodogram for TIC 279485093 and the light curve phased with $\nu_{\rm rot} = 0.080274\,{\rm d}^{-1}$. The vertical lines indicate frequencies in the literature.

tor 1 and 2 *TESS* data for this star have already been discussed by Cunha et al. (2019). Here we include additional data from sectors 3, 4, 6 and 7.

There is no clear indication of mean-light rotational modulation and the periodogram shows four peaks at $\nu_1 = 130.6585 \pm 0.0005$, $A_1 = 0.071 \pm 0.012$, $\nu_2 = 132.3660 \pm 0.0001$, $A_2 = 0.262 \pm 0.012$, $\nu_3 = 134.3358 \pm 0.0002$, $A_3 = 0.142 \pm 0.011$ and $\nu_4 = 135.1962 \pm 0.0004\,{\rm d}^{-1}$, $A_4 = 0.084 \pm 0.012$ ppt (Fig. 5). Cunha et al. (2019) found ν_2 and ν_3 with the suspicion that ν_4 might be present. The additional data confirm that ν_4 is indeed a real frequency and furthermore identifies previously undetected peaks at ν_1 and ν_5.

Table 3. Extracted frequencies (ν in ${\rm d}^{-1}$) and amplitudes (A in ppt) for TIC 279485093. The column, $\nu_{\rm lit}$ lists frequencies reported in the literature.

ID	$\nu_{\rm lit}$	ν	A
ν_{10}	220.580	220.991 ± 0.021	0.012 ± 0.005
ν_9	223.370	224.994 ± 0.015	0.016 ± 0.005
$\nu_9 + \nu_{\rm rot}$		225.080 ± 0.019	0.013 ± 0.005
ν_1	226.337	226.348 ± 0.006	0.043 ± 0.005
$\nu_1 + \nu_{\rm rot}$		226.434 ± 0.014	0.018 ± 0.005
ν_2	229.214	229.215 ± 0.002	0.105 ± 0.005
$\nu_2 + \nu_{\rm rot}$		229.300 ± 0.010	0.024 ± 0.005
ν_3	232.209	232.194 ± 0.002	0.159 ± 0.005
ν_4	235.081	235.064 ± 0.001	0.186 ± 0.005
$\nu_5 - \nu_{\rm rot}$		237.965 ± 0.014	0.017 ± 0.005
ν_5	238.092	238.040 ± 0.012	0.021 ± 0.005
ν_8	240.965		
ν_7	241.184	241.171 ± 0.007	0.038 ± 0.005
$\nu_7 + \nu_{\rm rot}$		241.249 ± 0.017	0.015 ± 0.005
ν_6	242.411	242.405 ± 0.008	0.033 ± 0.005
$\nu_6 + \nu_{\rm rot}$		242.476 ± 0.015	0.017 ± 0.005

4.5 TIC 268751602 (HD 12932)

The rapid light variations in this star were discovered by Schneider & Weiss (1990) and further studied by Schneider et al. (1992). Martinez et al. (1994) corrected the pulsation frequency to $124.0962\,{\rm d}^{-1}$. The difference was attributed to an incorrect choice of alias by Schneider & Weiss (1990).

The star was observed by *TESS* in sector 3. A single frequency of $124.0965 \pm 0.0006\,{\rm d}^{-1}$ with amplitude 0.628 ± 0.01 ppt is found (Fig. 5). There are no significant sidelobe peaks or mean light variation which may be attributed to rotation.

4.6 TIC 279485093 (HD 24712)

Kurtz (1981) discovered 6.15 min ($234\,{\rm d}^{-1}$) oscillations in this cool magnetic Ap star. Kurtz & Seeman (1983) analysed the light curve and found six nearly equally-spaced frequency peaks interpreted as high radial order overtones. The rotation frequency from mean-light variation was found to be $\nu_{\rm rot} = 0.080274 \pm 0.00002\,{\rm d}^{-1}$ (Kurtz & Marang 1987b). Later, Kurtz et al. (1989) found that all six frequencies are amplitude modulated with the rotation of the star. These frequencies, $\nu_{\rm lit}$, are listed in Table 3 with frequency numbering as adopted by Kurtz et al. (1989).

The frequency of ν_6 does not fit the predictions of asymptotic theory for high-frequency acoustic modes. Cunha (2001) showed that it can be understood if the effect of the magnetic field on the frequencies of the oscillations is taken into account and predicted that another mode should be present at a slightly lower frequency. The "missing mode" (ν_7 in Table 3) was indeed later discovered by Kurtz et al. (2002). Kurtz et al. (2005) confirmed the above rotational frequency and detected a new peak, ν_8. From radial velocity measurements, Mkrtichian & Hatzes (2005) added ν_9 and ν_{10}. A re-analysis of photometric observations indicates that variations in amplitude occur on a timescale of days (White et al. 2011).

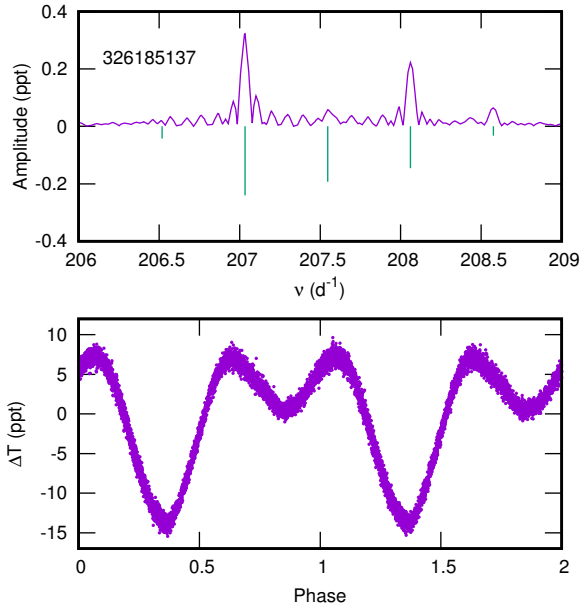

Figure 7. Periodogram for TIC 326185137 and the light curve phased with $\nu_{\rm rot} = 0.5137\,{\rm d}^{-1}$. The vertical lines show the frequency quintuplet (Kurtz et al. 1996) with lengths proportional to their amplitudes. Note the large change in relative amplitudes.

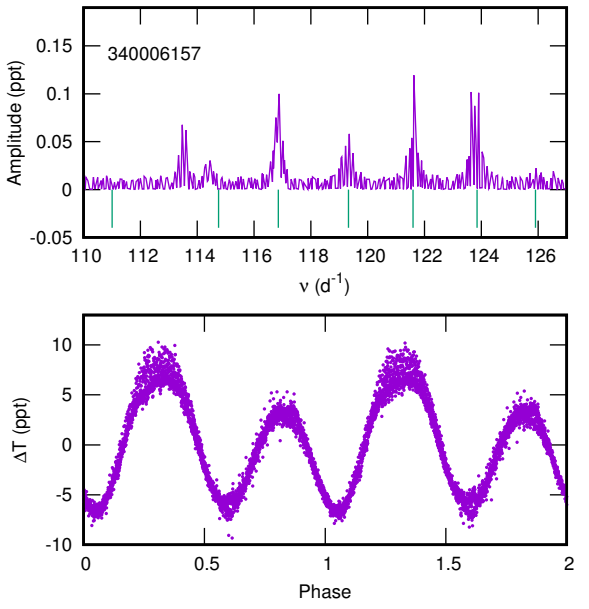

Figure 8. Periodogram for TIC 340006157 and the light curve phased with $\nu_{\rm rot} = 0.13015\,{\rm d}^{-1}$. The vertical lines below the periodogram show the frequencies listed in Matthews et al. (1987).

The star was observed for 26 d in sector 5. The periodogram peaks (Fig. 6) agree with frequencies found in the literature except that no match can be found for ν_8. Some rotational sidelobes can also be identified. The rotational light curve (Fig. 6) is somewhat distorted, but this is probably a result of the difficulty in correcting for the long-term trend in the data, since the observations barely cover two rotation periods.

4.7 TIC 326185137 (HD 6532)

Kurtz & Kreidl (1985) found a frequency triplet of 207.025, 207.541 and 208.018 $\rm d^{-1}$. Later, Kurtz et al. (1996) showed that the observations are fully described by a frequency quintuplet spaced exactly by the rotation frequency. The first and second harmonics are also visible. The central frequency is $\nu = 207.547069 \pm 0.000002\,{\rm d}^{-1}$ and the spacing is $\nu_{\rm rot} = 0.514145\,{\rm d}^{-1}$. Kurtz & Marang (1987a) refined the rotational frequency to $0.5140 \pm 0.0019\,{\rm d}^{-1}$.

The *TESS* light curve from sector 3 shows three peaks: 207.0320, 208.0620 and 208.5752 $\rm d^{-1}$ with uncertainties of about 0.0006 $\rm d^{-1}$. Although these frequencies are the same as found by Kurtz et al. (1996), the relative amplitudes are very different, as shown in Fig. 7. The relative amplitudes in roAp stars are often used to provide constraints on the geometry of the pulsation through the relation of Kurtz et al. (1990a):

$$\tan i \tan \beta = \frac{A^{(1)}_{+1} + A^{(1)}_{-1}}{A^{(1)}_{0}}$$

where $A^{(1)}_{\pm 1}$ are the dipole sidelobe amplitudes, $A^{(1)}_0$ is the amplitude of the central peak, i is the inclination angle and β is the angle between the rotational axis and the axis of pulsation. This holds true under the assumption of a pure, non-distorted, dipole mode ($l = 1$, $m = 0$), with sidelobes generated from rotation alone. Since the obliquity is unlikely to have changed over 25 yr, this must serve as a caution when using the above formula. The reason why the relative amplitudes are different in the *TESS* data and in the ground-based B data is not known.

The rotational peak in the *TESS* periodogram is strong with the first harmonic of almost the same amplitude. The best fit is $\nu_{\rm rot} = 0.5137 \pm 0.0003\,{\rm d}^{-1}$ (Fig. 7).

4.8 TIC 340006157 (HD 60435)

This star was discovered by Kurtz (1984). Matthews et al. (1987) detected 17 frequencies which were interpreted as consecutive radial overtones of $l = 1$ and $l = 2$ modes. These follow the asymptotic relationship with a large spacing of 25.8 μHz. They also found that certain oscillations can grow or decay from observable amplitudes in less than a day. The rotation frequency from the mean light was found to be $\nu_{\rm rot} = 0.1302\,{\rm d}^{-1}$ (Kurtz et al. 1990b).

The star was observed in sectors 3, 6 and 7 for a duration of 130 d with a 62-d gap between sectors 3 and 6. The periodogram of the combined data (Fig. 8) shows six peaks, each of which appears to contain fine structure. The mean light rotational curve has a frequency of $\nu_{\rm rot} = 0.13015 \pm 0.00002\,{\rm d}^{-1}$. None of the other peaks detected by Matthews et al. (1987) can be seen in the *TESS* data.

Periodograms of time sequences of duration of 1 d and overlap of 0.5 d were calculated to examine the development of the frequencies with time. Results are shown in Fig. 9. It is clear that the peaks have short lifetimes of the order of a day or two, confirming the findings reported by Matthews et al. (1987). Even more remarkable is the appearance and disappearance of some peaks between 114–120 $\rm d^{-1}$. For example, the peak of highest amplitude at about 116.7 $\rm d^{-1}$ dominates the frequency spectrum in days 6–12 but is not present at

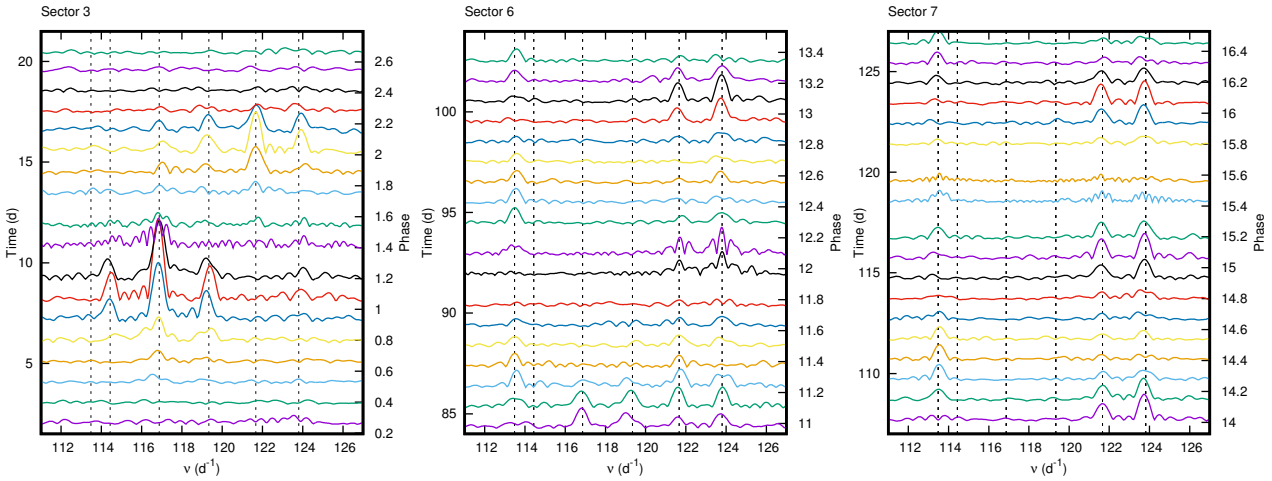

Figure 9. Periodograms of TIC 340006157 taken at intervals of one day showing the short-lived nature of the roAp pulsations. The vertical dotted lines show frequencies listed in Table 4. The left y-axis is the time in days relative to BJD 2458385 while the right y-axis is the rotational phase. The sector number for each panel is shown.

Table 4. Approximate frequencies (ν in d^{-1}) and amplitudes (A in ppt) for TIC 340006157.

ID	ν	A
$\nu_1 - \nu_{\rm rot}$	113.34	0.03
ν_1	113.47	0.07
$\nu_1 + \nu_{\rm rot}$	113.60	0.06
ν_2	114.43	0.03
ν_3	116.88	0.10
$\nu_4 - 2\nu_{\rm rot}$	119.08	0.04
$\nu_4 - \nu_{\rm rot}$	119.23	0.05
ν_4	119.34	0.06
$\nu_4 + \nu_{\rm rot}$	119.48	0.04
ν_5	121.62	0.12
$\nu_6 - \nu_{\rm rot}$	123.64	0.10
ν_6	123.76	0.09
$\nu_6 + \nu_{\rm rot}$	123.90	0.10

other times. In spite of the short-term nature of the variations, it is possible to discern the sidelobes due to rotational amplitude modulation in some cases. However, all peaks are broad with fine structure and poorly resolved. The approximate frequencies and amplitudes of those peaks which can be resolved are listed in Table 4.

4.9 TIC 350146296 (HD 63087)

This star was discovered by Cunha et al. (2019) to be a rapid oscillator from *TESS* sector 1–2 data. It is not known to be chemically peculiar. Analysis of the full data set (sectors 1–7; 190.8 d time span) allows the rotational frequency to be refined to $\nu_{\rm rot} = 0.375420 \pm 0.000017\,{\rm d}^{-1}$, which is the same, within the errors, as reported by Cunha et al. (2019) (Fig. 10). The extracted frequencies are listed in Table 5. In addition to the frequencies previously identified, two rotational sidelobes, $\nu_2 - 2\nu_{\rm rot}$ and $\nu_2 + 2\nu_{\rm rot}$, are found.

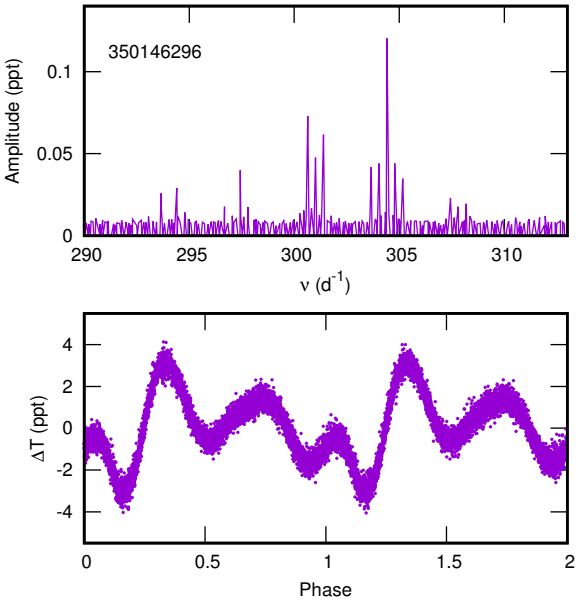

Figure 10. Periodogram of TIC 350146296 and the light curve phased with $\nu_{\rm rot} = 0.375420\,{\rm d}^{-1}$.

5 NEW ROAP STARS

In this section we list the new roAp stars discovered in the data from sectors 3 to 7. We include in this list only stars that satisfy one of the following criteria. Firstly, the star has been previously classified as Ap and the observed frequencies, and corresponding estimated radial orders, are typical of the known roAp stars. Secondly, the star has not previously been classified as Ap, but its frequencies and corresponding estimated radial orders are typical of roAp stars and there is evidence for Ap-like rotational modulation and/or pulsation multiplets split by integer values of the rotation frequency.

Table 5. Extracted frequencies (ν in d^{-1}) and amplitudes (A in ppt) for the total data set of TIC 350146296.

ID	ν	A
$\nu_1 - \nu_{\rm rot}$	293.6572 ± 0.0003	0.026 ± 0.003
$\nu_1 + \nu_{\rm rot}$	294.4081 ± 0.0003	0.029 ± 0.003
$\nu_2 - 2\nu_{\rm rot}$	296.6780 ± 0.0005	0.018 ± 0.003
ν_2	297.4294 ± 0.0002	0.041 ± 0.003
$\nu_2 + 2\nu_{\rm rot}$	297.8043 ± 0.0006	0.017 ± 0.003
$\nu_3 - \nu_{\rm rot}$	300.6411 ± 0.0001	0.074 ± 0.003
ν_3	301.0162 ± 0.0002	0.045 ± 0.003
$\nu_3 + \nu_{\rm rot}$	301.3916 ± 0.0001	0.063 ± 0.003
$\nu_4 - 2\nu_{\rm rot}$	303.6617 ± 0.0002	0.043 ± 0.003
$\nu_4 - \nu_{\rm rot}$	304.0368 ± 0.0002	0.042 ± 0.003
ν_4	304.4126 ± 0.0001	0.122 ± 0.003
$\nu_4 + \nu_{\rm rot}$	304.7880 ± 0.0002	0.042 ± 0.003
$\nu_4 + 2\nu_{\rm rot}$	305.1634 ± 0.0003	0.035 ± 0.003
$\nu_5 - \nu_{\rm rot}$	307.4341 ± 0.0004	0.023 ± 0.003
ν_5	307.8088 ± 0.0005	0.017 ± 0.003
$\nu_5 + \nu_{\rm rot}$	308.1848 ± 0.0005	0.020 ± 0.003

Table 6. Extracted frequencies (ν in d^{-1}) and amplitudes (A in ppt) for TIC 17676722.

ID	ν	A
$\nu_1 - 2\nu_{\rm rot}$	166.5000 ± 0.0012	0.151 ± 0.006
$\nu_1 - \nu_{\rm rot}$	167.1233 ± 0.0024	0.076 ± 0.006
ν_1	167.7495 ± 0.0003	0.621 ± 0.006
$\nu_1 + 2\nu_{\rm rot}$	168.9998 ± 0.0012	0.155 ± 0.006

5.1 TIC 17676722 (HD 63773)

This star was observed in sector 7 for 24.5 d. The mean light curve has a rotational frequency of $\nu_{\rm rot} = 0.6254 \pm 0.0002\,\mathrm{d}^{-1}$ (Fig. 11). There are four significant high-frequency peaks which can be interpreted as due to rotational amplitude modulation of a single oscillation at $167.7495\,\mathrm{d}^{-1}$ (Table 6, Fig. 11). Very little information is available for this star except for its spectral type of A2.

5.2 TIC 156886111 (HD 47284)

This is a known Ap star observed for a total of 48 d in sectors 6 and 7. The rotational frequency is given as $0.145859\,\mathrm{d}^{-1}$ by Watson et al. (2006), which agrees with the frequency derived from the *TESS* light curve (Fig. 12). There is an isolated peak at $5.4648\,\mathrm{d}^{-1}$ in the periodogram (Fig. 12) which is difficult to interpret. A list of the significant frequencies is shown in Table 7. The high frequencies consist of three oscillations and some rotationally modulated multiplets.

5.3 TIC 259587315 (HD 30849)

This is a known Ap star (ApSrCrEu). Hensberge et al. (1981) found a rotation period $\nu_{\rm rot} = 0.0631\,\mathrm{d}^{-1}$. Martinez & Kurtz (1994b) searched for roAp pulsations but none were detected.

Sector 4 and 5 observations show that this is a roAp star (Fig. 13). There are three well-separated peaks each of which shows fine structure which seems to be composed of rotationally-split components. Provisional identification of the most significant peaks are given in Table 8. More peaks are undoubtedly present, but these are poorly resolved due to the long rotation period. More data are required to verify the splitting to higher precision. The best fit to the mean light gives $\nu_{\rm rot} = 0.06319 \pm 0.00007\,\mathrm{d}^{-1}$ (Fig. 13).

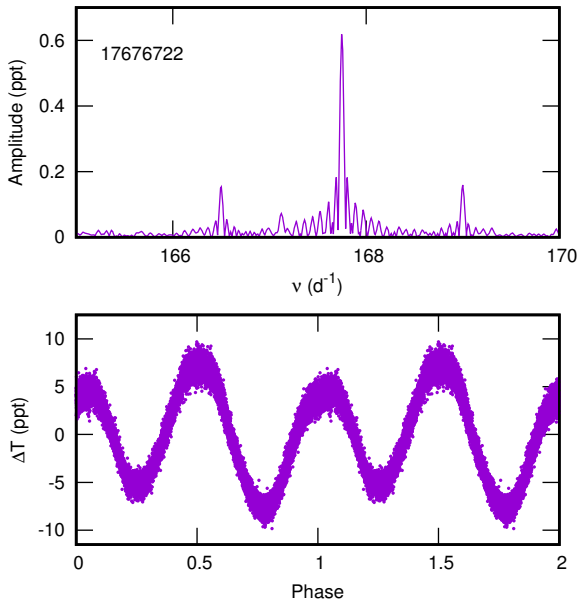

Figure 11. Periodogram of TIC 17676722 and the light curve phased with $\nu_{\rm rot} = 0.6254\,\mathrm{d}^{-1}$.

Table 7. Extracted frequencies (ν in d^{-1}) and amplitudes (A in ppt) for TIC 156886111.

ID	ν	A
ν_0	5.4648 ± 0.0004	0.340 ± 0.008
ν_1	110.1233 ± 0.0033	0.036 ± 0.008
$\nu_2 - \nu_{\rm rot}$	112.4111 ± 0.0021	0.057 ± 0.008
$\nu_2 + \nu_{\rm rot}$	112.7019 ± 0.0023	0.053 ± 0.008
$\nu_3 - 2\nu_{\rm rot}$	113.5693 ± 0.0022	0.055 ± 0.008
$\nu_3 - \nu_{\rm rot}$	113.7142 ± 0.0025	0.048 ± 0.008
ν_3	113.8591 ± 0.0011	0.109 ± 0.008
$\nu_3 + \nu_{\rm rot}$	114.0067 ± 0.0021	0.058 ± 0.008

Table 8. Extracted frequencies (ν in d^{-1}) and amplitudes (A in ppt) for the total data set of TIC 259587315.

ID	ν	A
ν_1	78.11065 ± 0.009	0.065 ± 0.040
ν_2	78.22939 ± 0.015	0.040 ± 0.040
$\nu_3 - 2\nu_{\rm rot}$	80.31933 ± 0.010	0.058 ± 0.040
ν_3	80.44372 ± 0.004	0.147 ± 0.040
$\nu_4 - \nu_{\rm rot}$	82.07746 ± 0.005	0.110 ± 0.040
ν_4	82.14120 ± 0.008	0.060 ± 0.040
$\nu_4 + \nu_{\rm rot}$	82.20437 ± 0.006	0.105 ± 0.040

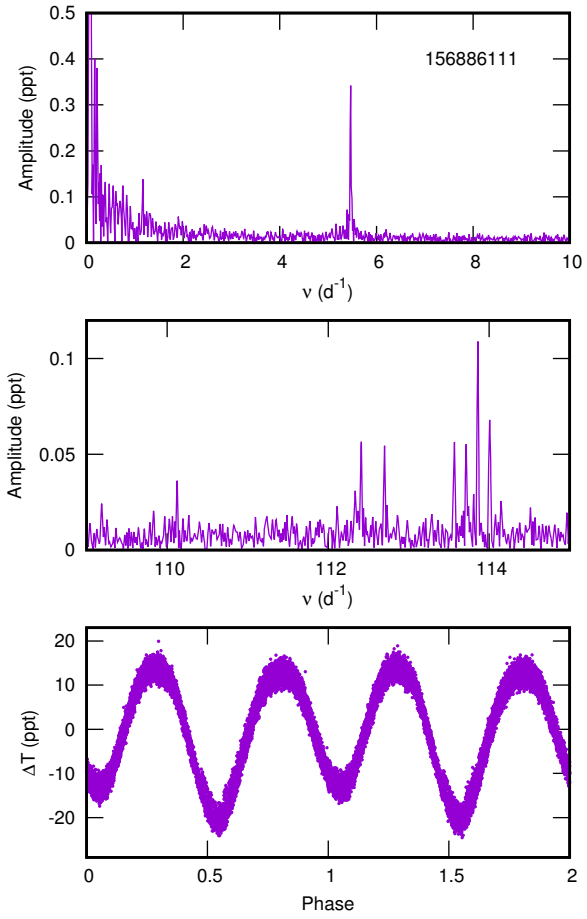

Figure 12. Periodograms of TIC 156886111 in the low-frequency region showing the isolated peak at $5.467\,\mathrm{d}^{-1}$ (top panel), with the middle panel showing the high-frequency range. The bottom panel is the light curve phased with $\nu_{\rm rot} = 0.1459\,\mathrm{d}^{-1}$.

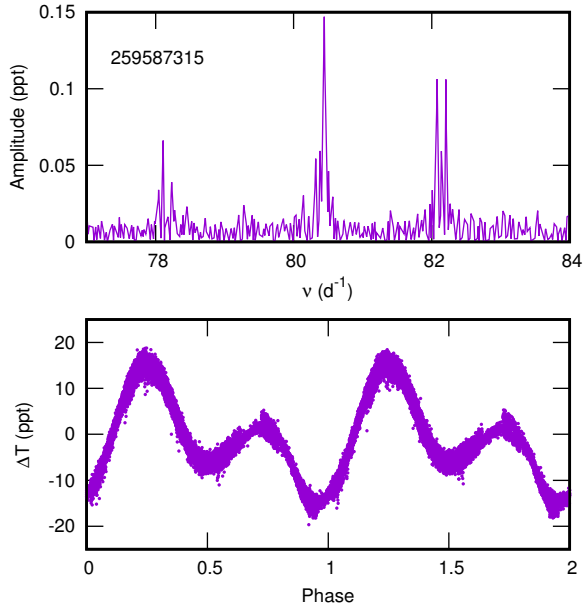

Figure 13. Periodogram of TIC 259587315 and the light curve phased with $\nu_{\rm rot} = 0.06319\,\mathrm{d}^{-1}$.

Table 9. Extracted frequencies (ν in d^{-1}) and amplitudes (A in ppt) for TIC 349945078.

ID	ν	A
$\nu_1 - \nu_{\rm rot}$	183.6431 ± 0.0007	0.103 ± 0.006
ν_1	183.7166 ± 0.0007	0.130 ± 0.006
$\nu_1 + \nu_{\rm rot}$	183.7920 ± 0.0010	0.071 ± 0.006
ν_2	188.9264 ± 0.0011	0.062 ± 0.006

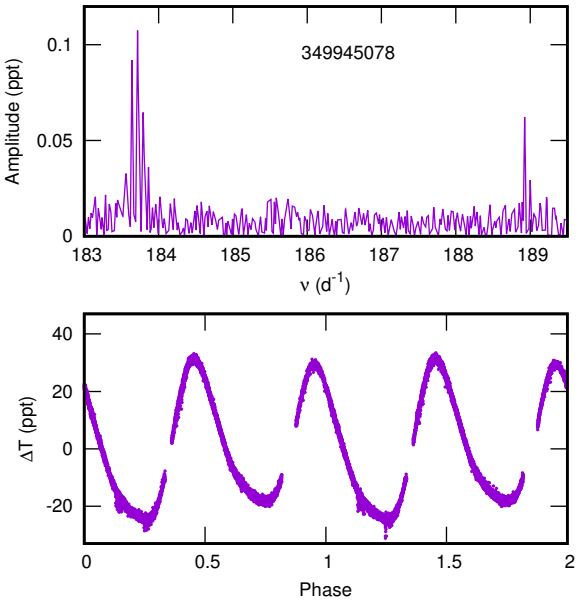

Figure 14. Periodogram of TIC 349945078 and the light curve phased with $\nu_{\rm rot} = 0.037103\,\mathrm{d}^{-1}$.

5.4 TIC 349945078 (HD 57040)

This is a known Ap star with $\nu_{\rm rot} = 0.037103\,\mathrm{d}^{-1}$ (Watson et al. 2006). It was observed for 47.8 d in sector 6 and 7. The mean light rotational frequency from the *TESS* data agrees with the published value. Because the time span of the *TESS* observations cover less than two rotation periods, the published value of $\nu_{\rm rot}$ was adopted. Fig. 14 shows the light curve phased with this frequency.

The high-frequency region shows two peaks, ν_1 and ν_2. The peak at ν_1 has structure which can just be resolved into the amplitude modulated components, as shown in Table 9. There is also a peak at $189.004\,\mathrm{d}^{-1}$ which is approximately $\nu_2 + \nu_{\rm rot}$, but this is only marginally significant.

6 CANDIDATE ROAP STARS

In addition to the new roAp stars discussed above and those published by Cunha et al. (2019), a number of A stars in *TESS* sectors 1 to 7 show a pulsation frequency spectrum that differs from that typically observed in δ Sct pulsators and, to varying degrees, resembles the pulsations in roAp stars. We classify them as candidate roAp stars if they exhibit pulsations with high frequencies that can be associated with high radial orders. High resolution spectroscopic observations of these stars should clarify if they are Ap or chemi-

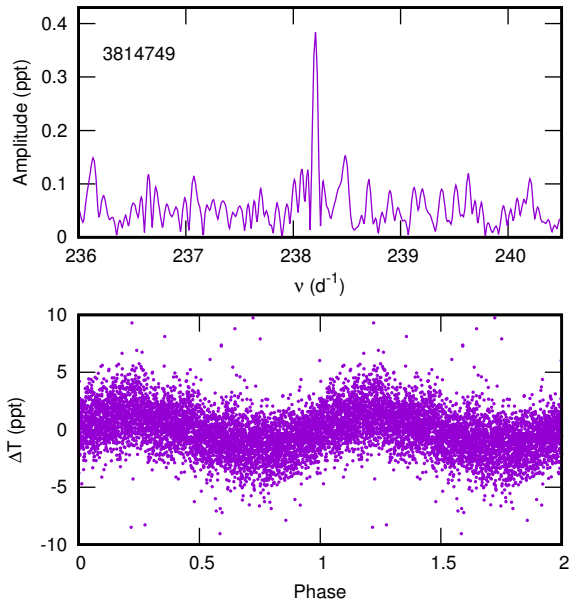

Figure 15. Periodogram of TIC 3814749 and the light curve phased with $\nu_{\rm rot} = 0.5920\,{\rm d}^{-1}$.

cally normal. If the latter is verified, and a different origin for the pulsations can be excluded (e.g., from contamination or binarity), then one will be led to the interesting conclusion that pulsations similar to those observed in roAp stars are excited in chemically normal, and possibly non-magnetic, stars.

6.1 TIC 3814749 (HD 3748)

This is a double star separated by 16.4 arcsec ($V = 9.61 + 9.88$ mag). The spectral types are given as A0/1 IV/V and A9/F0V: for the two components (Houk & Swift 1999). It was first classified as a detached eclipsing binary by Kazarovets et al. (1999) using Hipparcos photometry, but no period is listed. Using the same data, Koen & Eyer (2002) found it to be a variable of unknown type with a frequency $0.42482\,{\rm d}^{-1}$.

The star was observed for 20 d by *TESS* in sector 3. No evidence of an eclipse is seen. There is a low-frequency peak at $\nu = 0.592\,{\rm d}^{-1}$ which could be the rotational frequency, but this differs from the frequency found by Koen & Eyer (2002). A single high-frequency peak at $\nu = 238.205 \pm 0.003\,{\rm d}^{-1}$, amplitude $A = 0.385 \pm 0.042$ ppt is present (Fig. 15). The false-alarm probability is 10^{-12} and the S/N ratio is 12, indicating the presence of a real frequency. If the data are divided into two independent sets, the high frequency peak is present in both sets.

6.2 TIC 49818005 (HD 19687)

There is almost no information on this star except its spectral type A9 IV/V (Houk & Swift 1999). There is a single peak at $\nu = 141.8618 \pm 0.0008\,{\rm d}^{-1}$, amplitude $A = 0.246 \pm 0.009$ ppt (Fig. 16). The false-alarm probability is essentially zero and S/N = 31.

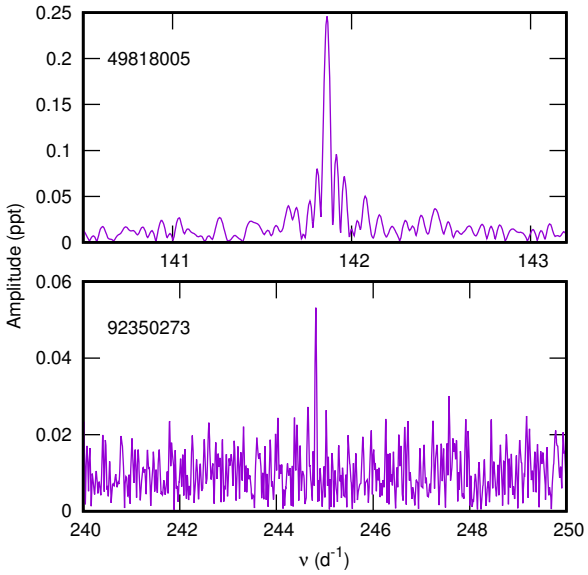

Figure 16. Periodograms for TIC 49818005 and TIC 92350273.

6.3 TIC 92350273 (CD-33 15279)

This is an F5 star. A literature search gives $T_{\rm eff}$ in the range 6000–7670 K. The *TESS* periodogram shows a single peak with $\nu = 244.813 \pm 0.003\,{\rm d}^{-1}$ and $A = 0.053 \pm 0.009$ ppt (Fig. 16). The S/N ratio of the peak is 9.2 while the false alarm probability is 2×10^{-4}.

6.4 TIC 220073982 (HD 288081)

The periodogram of this star shows two low-frequency peaks: a fundamental at $3.260 \pm 0.002\,{\rm d}^{-1}$ and the first harmonic which has a slightly higher amplitude. If this is interpreted as rotational modulation it would indicate very rapid rotation. While the parameters listed in Table 1 lead to a critical rotational frequency of about $2.8\,{\rm d}^{-1}$, it should be noted that the measured effective temperature will be smaller than the true $T_{\rm eff}$ owing to gravitational darkening at the equator caused by rapid rotation. A value of $T_{\rm eff} = 8500$ K, for example, leads to a critical rotational frequency of about $3.26\,{\rm d}^{-1}$. The light curve phased with $3.26\,{\rm d}^{-1}$ is shown in Fig. 17.

There are two significant high frequencies at $\nu_1 = 73.101 \pm 0.004$, $A_1 = 0.081 \pm 0.011$ and $\nu_2 = 69.841 \pm 0.005\,{\rm d}^{-1}$, $A_2 = 0.064 \pm 0.011$ ppt. Another peak at $\nu_3 = 79.620\,{\rm d}^{-1}$ and a fourth peak at $\nu_4 = 66.567\,{\rm d}^{-1}$ may be present. These form a quintuplet spaced by $3.260\,{\rm d}^{-1}$ with one missing peak and central frequency ν_1 (Fig. 17). The star closely resembles an amplitude modulated roAp star. It is not known to be chemically peculiar, and the short rotation period would make it the most rapidly-rotating object of this class. From the global parameters listed in Table 1, the observed frequencies correspond to a radial order $n \approx 19$, which is not uncommon in roAp stars.

In roAp stars the rotational amplitude modulation is a result of two different axes, rotation and magnetic, which are not aligned. Tidal modulation also leads to two non-aligned axes and thus to pulsational amplitude modulation (Balona 2018c). This may be an alternative explanation for

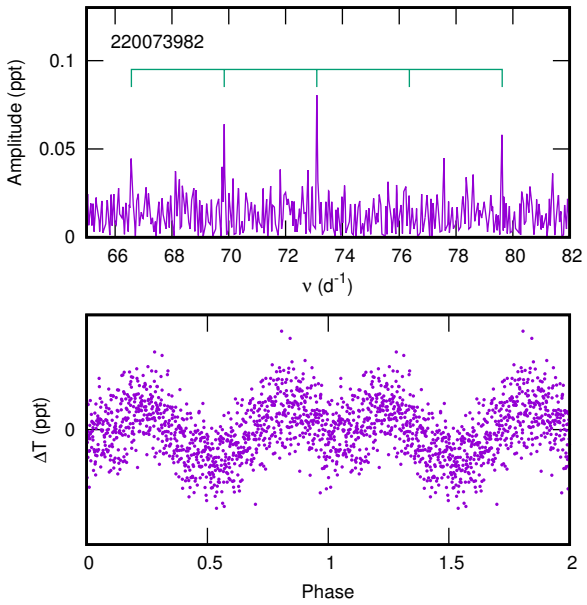

Figure 17. Periodogram of TIC 220073982 showing peaks spaced by $3.260\,\mathrm{d}^{-1}$. The light curve phased with $3.260\,\mathrm{d}^{-1}$ is shown in the bottom panel.

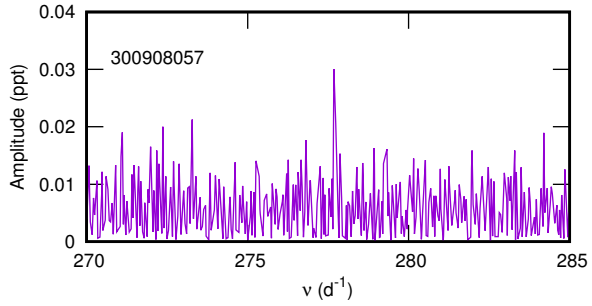

Figure 18. Periodogram for TIC 300908057.

the equally-spaced quintuplet in this star. If the $3.260\,\mathrm{d}^{-1}$ frequency is the orbital frequency, one may expect large radial velocity variations.

6.5 TIC 300908057 (HD 203997)

Almost nothing is known about this star except its spectral type, G1V. The TIC effective temperature, $T_{\rm eff}$ = 6174 K, places it at about F8. The periodogram shows a single peak at $\nu = 277.676 \pm 0.003\,\mathrm{d}^{-1}$, amplitude $A = 0.030 \pm 0.005$ ppt (Fig. 18). No other significant peak is present. The false alarm probability is quite high at 0.005 and S/N = 8.5. The star needs to be re-observed to confirm the reality of the high frequency. TIC 300908057 falls below the zero-age main sequence in Fig. 1, which might indicate that this is a subdwarf or other evolved object.

6.6 TIC 391892593 (HD 63037)

This is a known Am star. There is only a single peak at $\nu_1 = 148.3816 \pm 0.0005\,\mathrm{d}^{-1}$, $A_1 = 0.021 \pm 0.003$ ppt (Fig. 19). The S/N ratio is 9 and the false alarm probability is 3×10^{-4}.

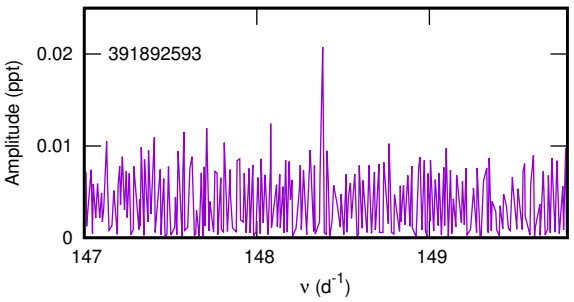

Figure 19. Periodogram of TIC 391892593.

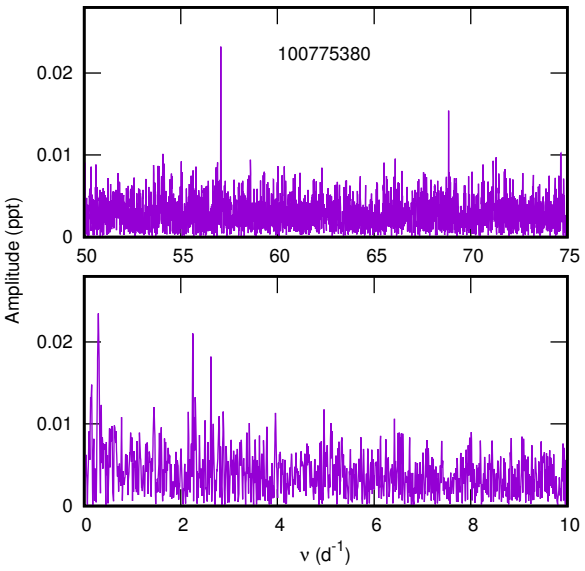

Figure 20. Periodograms of TIC 100775380 in two different frequency regions.

7 ADDITIONAL HIGH-FREQUENCY PULSATORS

Interestingly, there are stars whose oscillation spectra do not resemble that of a δ Sct star but whose frequencies, and associated radial orders, are lower than expected for a roAp star. These stars are describe in this section.

7.1 TIC 100775380 (HD 39763)

This is a close double (V = 8.44, 8.59 mag) with separation of 0.31 arcsec and combined A1V spectral type. It was observed in sectors 5 and 6 for a total of 52 d. The periodogram shows two peaks at $\nu_1 = 57.063 \pm 0.001$, $A_1 = 0.023 \pm 0.003$ and $\nu_2 = 68.860 \pm 0.002\,\mathrm{d}^{-1}$, $A_2 = 0.015 \pm 0.003$ ppt (Fig. 20). There are some barely significant peaks at low frequency suggesting γ Dor or SPB pulsations, but the star is far from the instability region of either of these two classes of pulsating stars. This is one of those stars that could well be classified as a δ Sct variable except for the unusual isolated pair of peaks.

Considering the global parameters indicated in Table1 and the observed frequencies, we estimate the radial orders

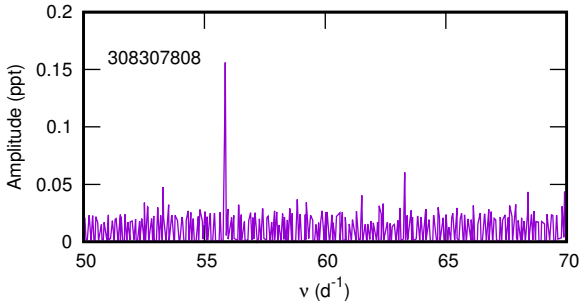

Figure 21. Periodogram of TIC 308307808.

of the modes to be around 11 and 13, which are smaller that those usually seen in roAp stars.

7.2 TIC 308307808 (CD-60 2021)

This A3/A5 star is a member of the open cluster NGC 2516. It was observed for 26 d in sector 4 and again for 24 d in sector 7 with a gap of 55 d between the two sets of data. The star is difficult to classify. There are two significant peaks at $\nu_1 = 55.8688 \pm 0.0003$, $A_1 = 0.157 \pm 0.009$ and $\nu_2 = 63.2935 \pm 0.0008\,\mathrm{d}^{-1}$, $A_2 = 0.061 \pm 0.009$ ppt, which are barely within the roAp range (Fig. 21). There is also a peak at $6.9227 \pm 0.0005\,\mathrm{d}^{-1}$, $A = 0.094 \pm 0.009$ ppt. These peaks are present in the individual sector 4 and sector 7 data sets. Perhaps the star can also be classified as an unusual δ Sct. Also, from the estimated global parameters these frequencies correspond to radial orders of around 11, which is smaller than found in roAp stars.

7.3 TIC 399665133 (BD+06 763)

This A2 star was observed for 26 d in sector 5. The highest peak in the periodogram is at $2.237 \pm 0.001\,\mathrm{d}^{-1}$ (Fig. 22) which we take to be the rotational frequency, but could also be a result of binarity. In addition, the periodogram shows a series of low-amplitude peaks of which the most significant are $\nu_1 = 52.078 \pm 0.002$, $A_1 = 0.087 \pm 0.007$, $\nu_2 = 58.636 \pm 0.002$, $A_2 = 0.078 \pm 0.007$, $\nu_3 = 71.102 \pm 0.003\,\mathrm{d}^{-1}$ and $A_3 = 0.047 \pm 0.007$ ppt. There is no clear relationship between these peaks and $\nu_{\rm rot}$ and there are no equal spacings. Also, the estimated radial order of the mode with largest amplitude is only $n = 11$.

7.4 TIC 407661867 (HD 37584)

This apparently non-Ap star was discovered to be rapidly oscillating by Cunha et al. (2019) but the significance of the oscillation was marginal. The additional data shows that there are, in fact, two peaks at $\nu_1 = 61.1287 \pm 0.0003$, $A_1 = 0.020 \pm 0.002$ and $\nu_2 = 64.0630 \pm 0.0002\,\mathrm{d}^{-1}$, $A_2 = 0.023 \pm 0.002$ ppt (Fig. 23). These frequencies are rather low compared to a typical roAp star. From the estimated global parameters, the radial order, $n \approx 9$, is also smaller than observed in known roAp stars.

There is also a low-frequency peak at $\nu_{\rm rot} = 1.7775 \pm 0.0002\,\mathrm{d}^{-1}$ which we assume is the rotational period. Because of the low amplitude, the light curve shown in Fig. 23 consists of averages in 1000 phase bins. In addition, there appear to be one or two low-amplitude peaks at even lower frequencies which might indicate a pulsational origin. As Cunha et al. (2019) point out, the field is quite crowded and the peaks might not originate in the same star.

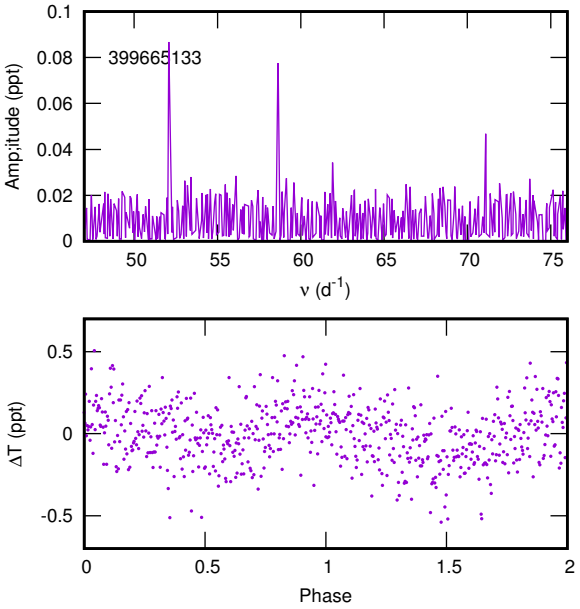

Figure 22. Periodogram of TIC 399665133 in the high frequency region. No other peaks are visible except for a single low-frequency peak at $\nu_{\rm rot} = 2.237\,\mathrm{d}^{-1}$. The light curve phased with $\nu_{\rm rot}$ is shown in the bottom panel.

Because we do not yet understand the mechanism which drives high-frequency pulsations in Ap stars and non-Ap stars, it is difficult to decide on a classification. We found several A–F stars with a small number of peaks at relatively high frequencies and nothing else of significance in the periodograms of the *TESS* data.

8 HIGH FREQUENCIES IN δ SCUTI STARS

In this section we discuss stars that exhibit pulsation frequencies typical of δ Sct stars. In addition, the periodograms have peaks with frequencies higher than usual for δ Sct stars which cannot be explained as combinations of lower frequency modes.

8.1 TIC 98728812 (HD 18407)

This A0V star (Houk & Smith-Moore 1988) shows a single frequency at $65.302 \pm 0.002\,\mathrm{d}^{-1}$, amplitude $A = 0.056 \pm 0.007$ ppt. The S/N ratio is 9.5 and the false alarm probability is 5×10^{-7}. The radial order for this frequency is $n \approx 11$. There is another peak at around $62\,\mathrm{d}^{-1}$, but it is not formally significant (Fig. 24). Apart from these, there are a few low-amplitude, but significant, peaks at low frequencies suggestive of γ Dor or δ Sct pulsations. The highest amplitude low-frequency peak is at $0.085\,\mathrm{d}^{-1}$. The peak at $5.552 \pm 0.003\,\mathrm{d}^{-1}$ has S/N = 8.8 and a false alarm probability of 4×10^{-7}.

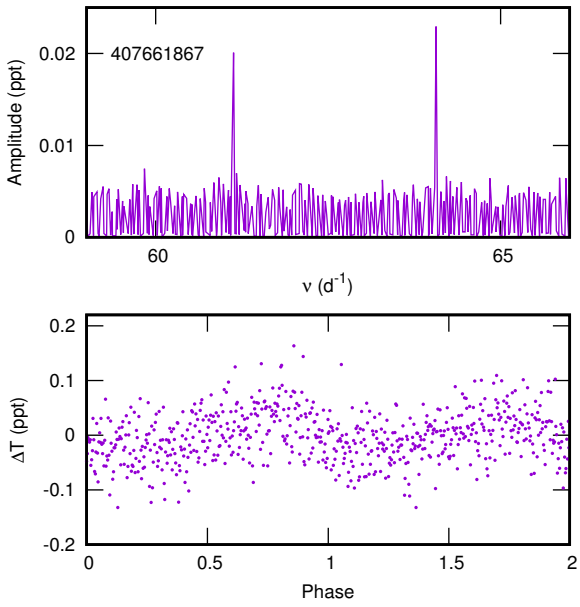

Figure 23. Periodogram of TIC 407661867 in the high frequency region. The light curve phased with $\nu_{\rm rot} = 1.777\,{\rm d}^{-1}$ is shown in the bottom panel.

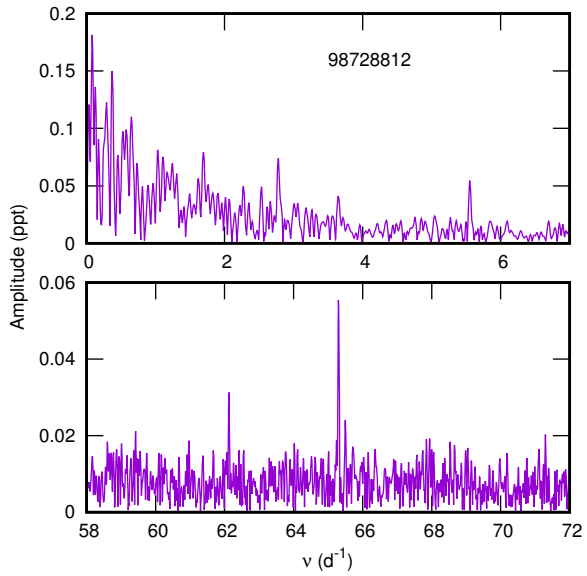

Figure 24. Periodogram of TIC 98728812 with some barely significant low-frequency peaks suggestive of a γ Dor variable and two high-frequency peaks (bottom panel).

8.2 TIC 302296720 (HD 203144)

This A5/7V star has a companion 3 mag fainter at a distance of 0.3 arcsec. It is a δ Sct star from which 24 significant frequencies can be extracted. Among them is an isolated high-frequency peak at $\nu = 82.831 \pm 0.004\,{\rm d}^{-1}$, amplitude $A = 0.037 \pm 0.005$ ppt, which is well within the roAp region (Fig. 25). This corresponds to radial order $n \approx 14$.

The question naturally arises whether this peak is a harmonic or combination of some of the peaks in the δ Sct range. To test this notion, combinations of the form $\nu = p\nu_i + q\nu_j$ were calculated with all possible choices of ν_i, ν_j selected from the 24 frequencies. Here p and q are positive and negative integers with $|p, q| \leq 5$. It should be noted that any frequency can be matched by a combination when $|p, q|$ and the matching tolerance are sufficiently large.

A matching tolerance of $0.04\,{\rm d}^{-1}$ was chosen, which is about an order of magnitude larger then the largest frequency error. This conservative error margin was chosen to ensure that any satisfactory combination frequency would certainly be detected. Even so, no combination was found and it appears that the high frequency is an independent mode.

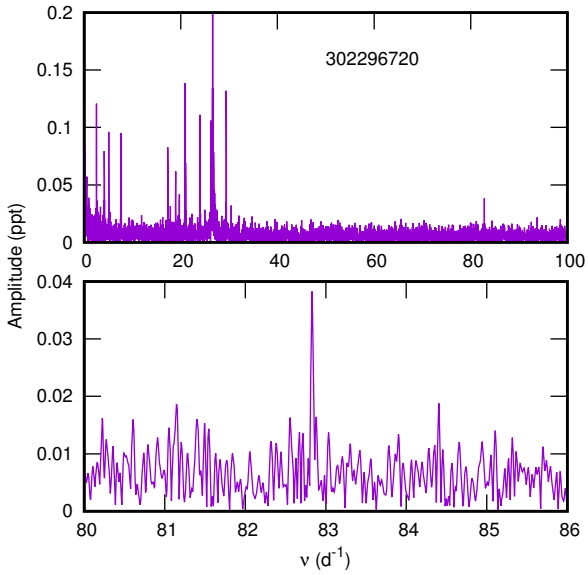

Figure 25. Periodogram of TIC 302296720 which appears to be a δ Scuti star with a single high frequency (bottom panel).

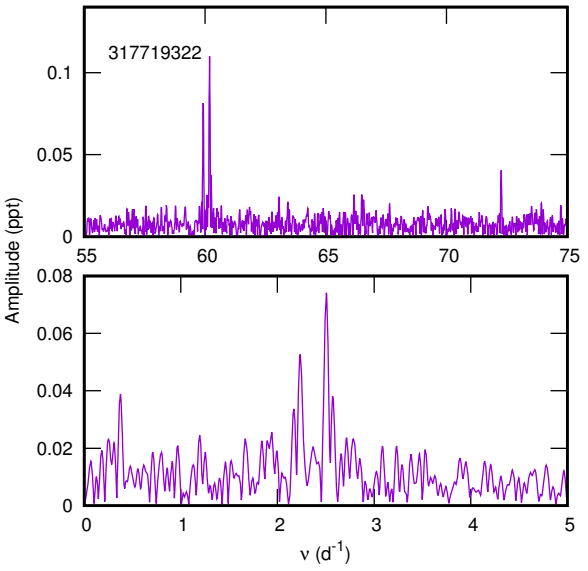

Figure 26. Periodograms of TIC 317719322 showing the high-frequency and the low-frequency regions.

8.3 TIC 317719322 (HD 40098)

This early A star was observed for 22 d in sector 6. The periodogram shows just a few peaks. The low-frequency region shows two peaks at 2.235 and 2.506 d^{-1} while the peaks in the high-frequency region are as follows: $\nu_1 = 60.189 \pm 0.001$, $A_1 = 0.110 \pm 0.006$; $\nu_2 = 59.927 \pm 0.002$, $A_2 = 0.079 \pm 0.006$; $\nu_3 = 72.263 \pm 0.004\,d^{-1}$, $A_3 = 0.041 \pm 0.006$ ppt (Fig. 26). It is difficult to classify this star, but it has been included in this section because of the two low frequencies which look like γ Dor modes. However, the spectral type, A2/3V, implies that the star is too hot for this variability class. Both the peaks at 2.234 ± 0.003 and $2.506 \pm 0.002\,d^{-1}$ are highly significant with S/N in the range 12–17 and false alarm probabilities of 10^{-9} and 10^{-25} respectively. The high frequencies fall within the roAp range, but the estimated radial orders are only around 9. There is no simple combination of frequencies which may account for any of the peaks.

8.4 TIC 439399707 (HD 225186)

The spectral type of this star is A1/2IV/V or A3V without any peculiarity. It was observed by Holdsworth et al. (2014) where it is classified as A5 and noted as a δ Sct star with pulsation frequencies exceeding 50 d^{-1}. There are 14 frequencies which can be extracted from the *TESS* data, as shown in Table. 10. Only one peak can be expressed as a combination: $\nu_{14} = 2\nu_8 - \nu_2$. The mean light of the star varies with frequency $\nu_{\rm rot} = 0.6016 \pm 0.0002\,d^{-1}$ (Fig. 27).

The estimated radial order of the highest frequency is only about 9 which is low compared to those for most known roAp stars. It is included here because the frequency distribution is very unusual for a δ Sct star. Also of interest are two flares which occur near maximum light at BJD 2458377.820 and BJD 2458380.000 (Fig. 27). Considering that this is quite a luminous star, the flares must be quite energetic. Taking the luminosity listed in Table 1 and integrating the flux underneath the flare, the energy released is estimated to be about 10^{36} ergs for each flare. Flares in active M dwarfs typically release 10^{33} – 10^{35} ergs (Schmidt et al. 2018). There is no other star visible within a radius of 2 arcmin. The star is identified with the *ROSAT* X-ray source 1RXS J000415.1-172524 (Voges et al. 1999).

The stars discussed above serve to show that in at least some δ Sct stars not all the high frequencies are explained as combination frequencies and that independent modes with frequencies as high as some of those found in roAp stars are present, though at typically smaller radial orders. It is also worth noting that we have found a few δ Sct stars in the *TESS* and *Kepler* data where the frequency spectrum consists of just a few closely-spaced peaks at relatively high frequencies and nothing else. These resemble the frequency spectrum of a typical roAp star, but at lower frequencies. It is not clear how such strange mode selection can occur.

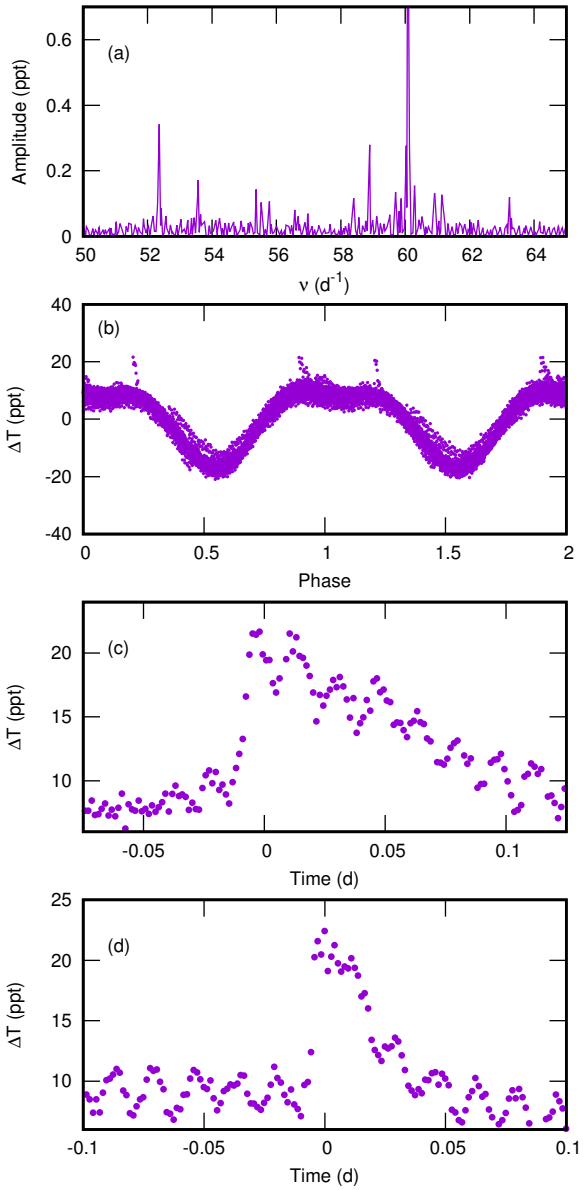

Figure 27. Panel (a): the periodogram of the δ Sct star TIC 439399707. No other peaks are present except for the low-frequency rotational peak and its harmonic. Panel (b) shows the light curve phased with frequency $\nu_{\rm rot} = 0.6016\,d^{-1}$. Two flaring events are seen near maximum light. These are shown in more detail in panels (c) and (d) where the time is relative to the flare maxima. Note the sinusoidal variations associated with the $60.079\,d^{-1}$ periodicity.

9 DISCUSSION AND CONCLUSIONS

Light curves and periodograms of over 18000 stars with $T_{\rm eff} \geq 6000$ K in *TESS* sectors 1–7 were visually examined. High-frequency peaks were found in several stars, not only among the chemically peculiar ApSrEuCr, but also among apparently chemically normal stars. All stars previously known to be roAp stars in the list of Smalley et al. (2015) were recovered. Some of these results have already been presented by Cunha et al. (2019).

Among the most interesting results discovered in the analysis of known roAp stars is the large change in relative amplitudes of the roAp peaks in TIC 326185137 (HD 6532). The relative amplitudes of the multiplets arising from amplitude modulation are often used to estimate the tilt of the pulsation axis relative to the rotation axis. The relative amplitudes derived in the *TESS* data are very different

Table 10. Extracted frequencies, ν (in d^{-1}), and amplitudes, A (in ppt), for TIC 439399707.

ID	ν	A
ν_1	52.363 ± 0.005	0.340 ± 0.017
ν_2	53.567 ± 0.011	0.170 ± 0.017
ν_3	55.368 ± 0.013	0.150 ± 0.017
ν_4	55.524 ± 0.024	0.083 ± 0.016
ν_5	55.777 ± 0.018	0.110 ± 0.016
ν_6	56.572 ± 0.025	0.078 ± 0.016
ν_7	56.976 ± 0.025	0.078 ± 0.016
ν_8	58.400 ± 0.024	0.083 ± 0.016
ν_9	58.890 ± 0.007	0.255 ± 0.017
ν_{10}	59.700 ± 0.015	0.127 ± 0.017
ν_{11}	60.079 ± 0.001	1.055 ± 0.018
ν_{12}	60.909 ± 0.013	0.148 ± 0.016
ν_{13}	61.136 ± 0.016	0.119 ± 0.016
ν_{14}	63.237 ± 0.017	0.112 ± 0.016

from those previously derived from ground-based B-band photometry. This requires an explanation and suggests that caution should be applied in using the amplitude formula.

Of particular interest is the confirmation that in at least one roAp star the mode lifetimes are no more than a few days. This is not an isolated case. The instability of the modes in KIC 8677585, for example, also indicates short mode lifetimes (Balona et al. 2013).

The search for roAp stars from ground-based observations has generally been confined to chemically peculiar SrEuCr stars and the theory that has been developed to account for the high frequencies relies on the large magnetic field that is associated with Ap stars. Observations from space have made it more feasible to broaden the search to normal stars. The *Kepler* mission has already produced a candidate, KIC 4840675 (Balona et al. 2012). This is an A7III or A5Vn δ Scuti variable with a dominant mode and many other modes of lower amplitude. It was independently classified as F0Vn by Niemczura et al. (2017) without mention of any chemical peculiarities. The most interesting aspect of this star is a triplet of independent modes in the range 118–129 d^{-1}, which is far outside the range of typical δ Sct frequencies.

Ground-based survey observations, such as *SuperWASP*, have also begun to uncover stars which are not classified as Ap but which show pulsations in the roAp range (Holdsworth et al. 2014). The *TESS* mission is proving that high-frequency light variations in stars not know to be Ap stars may be more common than previously thought. Of course, it may turn out that all stars with high frequencies are chemically peculiar when observed at sufficiently high spectroscopic resolution. The most pressing requirement at this time is to obtain spectra of these apparently non-peculiar stars with high frequencies in order to confirm whether they are chemically peculiar.

The huge variety in the distribution of frequency peaks in stars located in the same region of the H-R diagram is evident and cannot be explained by current models. It seems that pulsations in stars of intermediate mass are very sensitive to the physical conditions in the thin outer layers and that these differ from star to star, even for stars with the same effective temperature and luminosity, leading to similar stars exhibiting very different pulsation spectra (Balona 2018a,b). With the *TESS* survey, the different types of pulsators cohabiting this region of the H-R diagram may be studied with statistically sound samples. This will allow us to establish the similarities and differences underlying their pulsations and, potentially, shed light on the driving mechanisms.

ACKNOWLEDGMENTS

We thank V. Antoci, D. M. Bowman, G. Wade and O. Kochukhov for comments, useful discussions and suggestions. We also thank an anonymous referee for helpful comments.

LAB wishes to thank the National Research Foundation of South Africa for financial support. DLH acknowledges financial support from the Science and Technology Facilities Council (STFC) via grant ST/M000877/1. MC is supported by FCT - Fundação para a Ciência e a Tecnologia through national funds and by FEDER through COMPETE2020 - Programa Operacional Competitividade e Internacionalização by these grants: UID/FIS/04434/2019, PTDC/FIS-AST/30389/2017 & POCI-01-0145-FEDER-030389 & CEECIND/02619/2017.

This paper includes data collected by the *TESS* mission. Funding for the *TESS* mission is provided by the NASA Explorer Program. Funding for the *TESS* Asteroseismic Science Operations Centre is provided by the Danish National Research Foundation (Grant agreement no.: DNRF106), ESA PRODEX (PEA 4000119301) and Stellar Astrophysics Centre (SAC) at Aarhus University. We thank the *TESS* and TASC/TASOC teams for their support of the present work.

This work has made use of data from the European Space Agency (ESA) mission Gaia (`https://www.cosmos.esa.int/gaia`), processed by the Gaia Data Processing and Analysis Consortium (DPAC, `https://www.cosmos.esa.int/web/gaia/dpac/consortium`). Funding for the DPAC has been provided by national institutions, in particular the institutions participating in the Gaia Multilateral Agreement.

This research has made use of the SIMBAD database, operated at CDS, Strasbourg, France.

The data presented in this paper were obtained from the Mikulski Archive for Space Telescopes (MAST). STScI is operated by the Association of Universities for Research in Astronomy, Inc., under NASA contract NAS5-2655.

REFERENCES

Antoci V., Cunha M., Houdek G., et al., 2014, ApJ, 796, 118
Balmforth N. J., Cunha M. S., Dolez N., Gough D. O., Vauclair S., 2001, MNRAS, 323, 362
Balona L. A., 2013, MNRAS, 431, 2240
—, 2017, MNRAS, 467, 1830
—, 2018a, MNRAS, 479, 183
—, 2018b, Front. Astron. Space Sci., 5:43
—, 2018c, MNRAS, 476, 4840
Balona L. A., Breger M., Catanzaro G., et al., 2012, MNRAS, 424, 1187
Balona L. A., Catanzaro G., Crause L., et al., 2013, MNRAS, 432, 2808

Bertelli G., Girardi L., Marigo P., Nasi E., 2008, A&A, 484, 815
Bigot L., Dziembowski W. A., 2002, A&A, 391, 235
Bowman D. M., 2017, Amplitude Modulation of Pulsation Modes in Delta Scuti Stars
Bowman D. M., Kurtz D. W., 2018, MNRAS, 476, 3169
Chandler C. O., McDonald I., Kane S. R., 2016, AJ, 151, 59
Cunha M. S., 2001, MNRAS, 325, 373
—, 2002, MNRAS, 333, 47
—, 2006, MNRAS, 365, 153
Cunha M. S., Antoci V., Holdsworth D. L., et al., 2019, MNRAS, submitted
Cunha M. S., Gough D., 2000, MNRAS, 319, 1020
Cunha M. S., Théado S., Vauclair S., 2004, in IAU Symposium, Vol. 224, The A-Star Puzzle, Zverko J., Ziznovsky J., Adelman S. J., Weiss W. W., eds., pp. 359–365
Dziembowski W. A., Goode P. R., 1996, ApJ, 458, 338
Eker Z., Soydugan F., Soydugan E., et al., 2015, AJ, 149, 131
Elkin V., Kurtz D. W., Mathys G., 2008, Contributions of the Astronomical Observatory Skalnate Pleso, 38, 317
Gaia Collaboration, Brown A. G. A., Vallenari A., Prusti T., de Bruijne J. H. J., Babusiaux C., Bailer-Jones C. A. L., 2018, ArXiv e-prints
Gaia Collaboration, Prusti T., de Bruijne J. H. J., et al., 2016, A&A, 595, A1
Gautschy A., Saio H., Harzenmoser H., 1998, MNRAS, 301, 31
Ghazaryan S., Alecian G., Hakobyan A. A., 2018, MNRAS, 480, 2953
Gontcharov G. A., 2017, Astronomy Letters, 43, 472
Gruberbauer M., Huber D., Kuschnig R., et al., 2011, A&A, 530, A135
Hartmann M., Hatzes A. P., 2015, A&A, 582, A84
Hensberge H., Maitzen H. M., Deridder G., et al., 1981, A&AS, 46, 151
Holdsworth D. L., Saio H., Sefako R. R., Bowman D. M., 2018, MNRAS, 480, 2405
Holdsworth D. L., Smalley B., Gillon M., et al., 2014, MNRAS, 439, 2078
Houk N., Smith-Moore M., 1988, Michigan Catalogue of Two-dimensional Spectral Types for the HD Stars. Volume 4.
Houk N., Swift C., 1999, in Michigan Spectral Survey, Ann Arbor, Dep. Astron., Univ. Michigan, Vol. 5, p. 0 (1999), Vol. 5, p. 0
Jenkins J. M., Twicken J. D., McCauliff S., et al., 2016, in Proc. SPIE, Vol. 9913, Software and Cyberinfrastructure for Astronomy IV, p. 99133E
Kazarovets E. V., Samus N. N., Durlevich O. V., Frolov M. S., Antipin S. V., Kireeva N. N., Pastukhova E. N., 1999, Information Bulletin on Variable Stars, 4659
Kochukhov O., Bagnulo S., Barklem P. S., 2002, ApJ, 578, L75
Koen C., Eyer L., 2002, MNRAS, 331, 45
Kounkel M., Covey K., Suárez G., et al., 2018, AJ, 156, 84
Kunder A., Kordopatis G., Steinmetz M., et al., 2017, AJ, 153, 75
Kurtz D. W., 1978, Information Bulletin on Variable Stars, 1436, 1
—, 1981, Information Bulletin on Variable Stars, 1915
—, 1982, MNRAS, 200, 807
—, 1984, MNRAS, 209, 841
Kurtz D. W., Cameron C., Cunha M. S., et al., 2005, MNRAS, 358, 651
Kurtz D. W., Hubrig S., González J. F., van Wyk F., Martinez P., 2008, MNRAS, 386, 1750
Kurtz D. W., Kawaler S. D., Riddle R. L., et al., 2002, MNRAS, 330, L57
Kurtz D. W., Kreidl T. J., 1985, MNRAS, 216, 987
Kurtz D. W., Marang F., 1987a, MNRAS, 228, 141
—, 1987b, MNRAS, 229, 285
Kurtz D. W., Martinez P., Koen C., Sullivan D. J., 1996, MNRAS, 281, 883
Kurtz D. W., Martinez P., Tripe P., 1994, MNRAS, 271, 421
Kurtz D. W., Matthews J. M., Martinez P., et al., 1989, MNRAS, 240, 881
Kurtz D. W., Seeman J., 1983, MNRAS, 205, 11
Kurtz D. W., Shibahashi H., Goode P. R., 1990a, MNRAS, 247, 558
Kurtz D. W., van Wyk F., Marang F., 1990b, MNRAS, 243, 289
Martinez P., Kurtz D. W., 1994a, MNRAS, 271, 118
—, 1994b, MNRAS, 271, 129
Martinez P., Kurtz D. W., Ashley R., 1993, Information Bulletin on Variable Stars, 3844
Martinez P., Kurtz D. W., van Wyk F., 1994, MNRAS, 271, 305
Matthews J. M., Kurtz D. W., Wehlau W. H., 1987, ApJ, 313, 782
McDonald I., Zijlstra A. A., Watson R. A., 2017, MNRAS, 471, 770
Mkrtichian D. E., Hatzes A. P., 2005, A&A, 430, 263
Muñoz Bermejo J., Asensio Ramos A., Allende Prieto C., 2013, A&A, 553, A95
Netopil M., Paunzen E., Hümmerich S., Bernhard K., 2017, MNRAS, 468, 2745
Niemczura E., Polińska M., Murphy S. J., et al., 2017, MNRAS, 470, 2870
Pecaut M. J., Mamajek E. E., 2013, ApJS, 208, 9
Perraut K., Brandão I., Cunha M., Shulyak D., Mourard D., Nardetto N., ten Brummelaar T. A., 2016, A&A, 590, A117
Ricker G. R., Winn J. N., Vanderspek R., et al., 2015, Journal of Astronomical Telescopes, Instruments, and Systems, 1, 014003
Ryabchikova T., Sachkov M., Kochukhov O., Lyashko D., 2007, A&A, 473, 907
Saio H., 2005, MNRAS, 360, 1022
—, 2014, in IAU Symposium, Vol. 301, Precision Asteroseismology, Guzik J. A., Chaplin W. J., Handler G., Pigulski A., eds., pp. 197–204
Saio H., Gautschy A., 2004, MNRAS, 350, 485
Saio H., Kurtz D. W., Murphy S. J., Antoci V. L., Lee U., 2018, MNRAS, 474, 2774
Saio H., Ryabchikova T., Sachkov M., 2010, MNRAS, 403, 1729
Samus N. N., Durlevich O. V., et al., 2009, VizieR Online Data Catalog, 1, 2025
Scargle J. D., 1982, ApJ, 263, 835
Schmidt S. J., Shappee B. J., van Saders J. L., et al., 2018, arXiv e-prints
Schneider H., Kreidl T. J., Weiss W. W., 1992, A&A, 257, 130
Schneider H., Weiss W. W., 1990, Information Bulletin on Variable Stars, 3520
Smalley B., Niemczura E., Murphy S. J., et al., 2015, MNRAS, 452, 3334
Sousa S. G., Cunha M. S., 2008, MNRAS, 386, 531
Stassun K. G., Oelkers R. J., Pepper J., et al., 2018, AJ, 156, 102
Stevens D. J., Stassun K. G., Gaudi B. S., 2017, AJ, 154, 259
Voges W., Aschenbach B., Boller T., et al., 1999, A&A, 349, 389
Watson C. L., Henden A. A., Price A., 2006, Society for Astronomical Sciences Annual Symposium, 25, 47
White T. R., Bedding T. R., Stello D., Kurtz D. W., Cunha M. S., Gough D. O., 2011, MNRAS, 415, 1638
Xiong D. R., Deng L., Zhang C., Wang K., 2016, MNRAS, 457, 3163